Journal of Hydrology 660 (2025) 133384

Contents lists available at ScienceDirect

Journal of Hydrology

journal homepage: www.elsevier.com/locate/jhydrol

Applications of percolation-based effective-medium approximation to electrical conductivity in porous media with surface conduction

David McLachlan [a], Meysam Ramezani [b], Robert Horton [c], Behzad Ghanbarian [d,e,f,*]

[a] School of Physics, University of the Witwatersrand, Johannesburg 2050, South Africa
[b] Division of Research and Development, Kariz Ab Kavosh Company, Tehran, Iran
[c] Department of Agronomy, Iowa State University, Ames IA 50011, United States
[d] Department of Earth and Environmental Sciences, University of Texas at Arlington, Arlington TX 76019, United States
[e] Department of Civil Engineering, University of Texas at Arlington, Arlington TX 76019, United States
[f] Division of Data Science, College of Science, University of Texas at Arlington, Arlington TX 76019, United States

ARTICLE INFO

Keywords:
Electrical conductivity
Critical water saturation
Percolation
Saturation

ABSTRACT

Electrical conductivity, σ, has been widely used to estimate hydraulic conductivity in porous media as well as to interpret subsurface low- and high-conductivity zones. σ in a porous medium is impacted by the complicated relationship between the surface conductivity of solids, as the low-conductivity component which is significant at dry conditions, and bulk conductivity through the pore space, as the high conductivity component. As water saturation increases from completely dry to fully saturated, the effect of the bulk conductivity on electrical conductivity substantially increases. In this study, for the first time, we propose applications of a percolation-based effective-medium approximation (P-EMA) to describe the saturation dependence of σ in porous media with significant surface conduction. The proposed P-EMA model estimates were compared to 16 data sets including three numerically simulated sets and thirteen measured sets. There was substantial agreement between the theory and the data, with scaling exponents ranging from 0.18 to 2.39, indicating non-universal behavior. The saturation-dependent σ values of packed clay loam soil samples were estimated with the P-EMA model. The P-EMA estimated values were in reasonable agreement with the measured values.

1. Introduction

Electrical conductivity, σ, is a fundamental property of porous media with broad applications in geophysics and environmental engineering. For instance, electrical resistivity tomography, as a non-destructive near-surface geophysical approach, has been widely used to predict soil erodibility (Karim and Tucker-Kulesza, 2018) and landslides (Perrone et al., 2014), aquifer characterization (Doetsch et al., 2012), and underground cavity detection (Martínez-Pagán et al., 2013). Resistivity logs have also been routinely applied in petroleum exploration for reservoir characterization (Tiab and Donaldson, 2024). Therefore, understanding and modeling electrical conductivity and/or resistivity is an active subject of research.

The electrical conductivity of porous materials is controlled by several factors, such as pores and their distribution (Ewing and Hunt, 2006), pore connectivity (Li et al., 2015), presence and saturation level of liquids within pores (Ghanbarian and Sahimi, 2017) as well as minerals and their charges (Leroy and Revil, 2009). In most porous media, particularly clay-rich ones (Waxman and Smits, 1968; Qi and Wu, 2022), electrical conductivity consists of more than one conducting phase (e.g., solid and liquid phases of known conductivities). Bulk conduction refers to the movement of charge carriers (e.g., ions or electrons) through the pore space, while surface conduction refers to charged surfaces and electrical double layer regions near the solid–liquid interface (Revil and Glover, 1997). Bulk conduction is predominantly determined by pore space properties and the conductivity of pore liquid. Surface conduction, however, is influenced by the solid matrix and its surface charge characteristics as well as ionic concentration and pH of the pore liquid. The formation of an electrical double layer (EDL) at the solid–liquid interface is crucial for surface conduction, as it facilitates the accumulation of charge carriers at the interface (Revil and Glover, 1998). Therefore, simple models (e.g., Archie, 1942) based on one conducting phase (or insulator-conductor systems) are inapplicable to porous media like soils and rocks with significant surface

* Corresponding author at: Department of Earth and Environmental Sciences, University of Texas at Arlington, Arlington TX 76019, United States.
E-mail address: ghanbarianb@uta.edu (B. Ghanbarian).

https://doi.org/10.1016/j.jhydrol.2025.133384
Received 22 March 2025; Received in revised form 18 April 2025; Accepted 23 April 2025
Available online 24 April 2025

conductions (or conductor-conductor systems).

Various theories have been developed to model σ in porous media. One of the early electrical conductivity models proposed for fine-grained or clay-rich media with significant surface conduction was developed by Waxman and Smits (1968). In their model electrical conductivity, σ, depends on water (or brine) conductivity, σ_w, as well as cation exchange capacity. In clay-free media with negligible surface-ions mobility and surface conductivity, σ is a linear function of σ_w (Archie, 1942). In clay-rich media, however, σ is a nonlinear function of σ_w at lower σ_w values, which then becomes a linear function of σ_w at higher σ_w values (Waxman and Smits, 1968; Johnson and Sen, 1988).

Theoretical models based on various approaches, such as self-consistent approximation (Landauer, 1952; Hashin, 1968; Sen et al., 1981), effective-medium theory (Sahimi, 1995; Richesson and Sahimi, 2021), percolation theory (Ewing and Hunt, 2006), were used to model σ in porous media and other materials with two conductive components. For instance, to model σ in media with considerable surface conduction using percolation theory, Ewing and Hunt (2006) assumed that bulk conduction through pore space and surface conduction through solid phase occur in parallel. Using a percolation-based effective medium approximation approach, McLachlan (1985) derived a single-exponent phenomenological equation, and Wu and McLachlan (1997) derived a two-exponent phenomenological equation. Although the percolation-based effective medium approximation has been used to model the saturation dependence of thermal conductivity in porous media (Ghanbarian and Daigle, 2016) or permeability in matrix-fracture geologic formations (Agbaje et al., 2023), to the best of our knowledge it has not been applied to model σ in variably saturated porous media. Therefore, the main objectives of this study are to: (1) apply percolation-based effective medium approximation to model saturation-dependent σ in media with significant surface conduction, (2) evaluate the proposed model using both numerically simulated values and measured values from the literature, and (3) assess its ability to estimate σ of a clay loam soil.

2. Percolation-based effective-medium approximation

In the literature, both percolation theory (Last and Thouless, 1971; Zhou et al., 1997; Ghanbarian et al., 2014; Ghanbarian and Berg, 2017) and the effective-medium approximation (Sahimi et al., 1983; Sen, 1997; Sahimi, 2023) have been widely used to model electrical conductivity in porous media. Percolation theory is applicable to insulator-conductor or conductor-superconductor systems, where the conductivity ratio (insulator to conductor or conductor to superconductor) is effectively zero. In contrast, the effective-medium approximation applies to systems composed of one, two or more conducting phases but provides accurate results primarily in homogeneous and relatively heterogeneous porous media (Adler and Berkowitz, 2000; Sahimi, 2011). To address these limitations, McLachlan (1987) combined concepts of percolation theory and effective-medium approximation to develop the following equation describing the electrical conductivity, σ, in media composed of low- and high-conductivity (σ_l and σ_h) components:

$$(1-f_h)\frac{\sigma_l^{1/t}-\sigma^{1/t}}{\sigma_l^{1/t}+\left(\frac{1-f_{hc}}{f_{hc}}\right)\sigma^{1/t}}+f_h\frac{\sigma_h^{1/t}-\sigma^{1/t}}{\sigma_h^{1/t}+\left(\frac{1-f_{hc}}{f_{hc}}\right)\sigma^{1/t}}=0 \quad (1)$$

where t is the critical scaling exponent, f_h is the fraction of the high-conductivity component and f_{hc} is the critical fraction of f_h. At values larger than f_{hc}, the conductivity σ is primarily due to the high-conductivity component (clusters) forming the σ_h component. Below f_{hc}, however, σ is mainly controlled by the conductivity of the low-conductivity component σ_l. Percolation-based effective-medium approximation (P-EMA), Eq. (1), is also known as the single exponent phenomenological percolation equation (McLachlan, 2021). Eq. (1) with $t=1$ and $f_{hc}=\frac{2}{Z}$ in which Z represents the coordination number reduces to the effective medium approximation. It also reduces to the power-law scaling from percolation theory when $\sigma_l=0$.

For a variably-saturated porous medium, schematically shown in Fig. 1, electrical conductivity occurs through the (i) pore space filled by a water-based solution and/or (ii) charged surfaces and electrical double layer region near the solid–liquid interface. Although the former has a dominant role above some critical water saturation, S_{wc}, the latter's contribution becomes more significant at water saturations below the S_{wc}.

Due to spatial heterogeneity (e.g., pores of different sizes), electrical conductance spatially varies within a porous medium. Under variably-saturated conditions, the lowest effective electrical conductivity occurs when a medium is completely dry, while the largest one occurs when the medium is fully saturated (Fig. 1). By replacing σ_l, σ_h and f_{hc} with respectively σ_{dry}, σ_{sat} and S_{wc}, the P-EMA, Eq. (1), can be rewritten as

$$(1-S_w)\frac{\sigma_{dry}^{1/t}-\sigma^{1/t}}{\sigma_{dry}^{1/t}+\left(\frac{1-S_{wc}}{S_{wc}}\right)\sigma^{1/t}}+S_w\frac{\sigma_{sat}^{1/t}-\sigma^{1/t}}{\sigma_{sat}^{1/t}+\left(\frac{1-S_{wc}}{S_{wc}}\right)\sigma^{1/t}}=0 \quad (2)$$

where σ_{dry} and σ_{sat} represent the electrical conductivity under completely dry and fully saturated conditions, respectively. For $\sigma_{dry}=0$, Eq. (2) reduces to the power-law scaling law from percolation theory i.e., $\sigma=\sigma_{sat}[(S_w-S_{wc})/(1-S_{wc})]^t$ (Ewing and Hunt, 2006).

3. Materials and Methods

In this section, first we briefly describe the experiments used to obtain measured and numerically simulated values used to evaluate the percolation-based effective-medium approximation. Then, we explain how Eqs. (1) and (2) are fitted to the data and how their parameters are determined.

3.1. Numerical simulations and Physical experiments

3.1.1. Gostick and Weber (2015) dataset

Gostick and Weber (2015) performed three-dimensional electrical conductivity simulations in two types of percolation resistor networks: (1) site and (2) bond. In the site percolation network, conductivity occurred between two sites if they were both conductors (i.e., all nearest conducting sites were linked). The conductivity of the low- and high-conductivity components were set equal to 10^{-3} and 10^2 S/m, respectively. More specifically, the electrical flow of current I between nodes i and j was considered to be proportional to the electrical conductance between them, g_{ij}, and the voltage difference, ΔV, i.e.

$$I=g_{ij}\Delta V \quad (3)$$

The summation of entering and existing electric currents at each node was set equal to zero to ensure steady-state conditions i.e.

$$\sum_{k=1}^{n}g_{ik}(V_k-V_i)=0 \quad (4)$$

where node i has n neighbors. For a network with N nodes, Gostick and Weber (2015) applied voltage boundary conditions on two opposing faces of the network and solved a linear system of N equations to calculate the voltage at each node and the total electrical flow through the network. Then, Ohm's law was used to determine resistivity and ultimately electrical conductivity through the network. The data used in this study were digitized from Fig. 4 of Gostick and Weber (2015). For this purpose, we used the DigitizeIt software package.

3.1.2. Ewing and Hunt (2006) dataset

The Ewing and Hunt (2006) dataset includes measured and

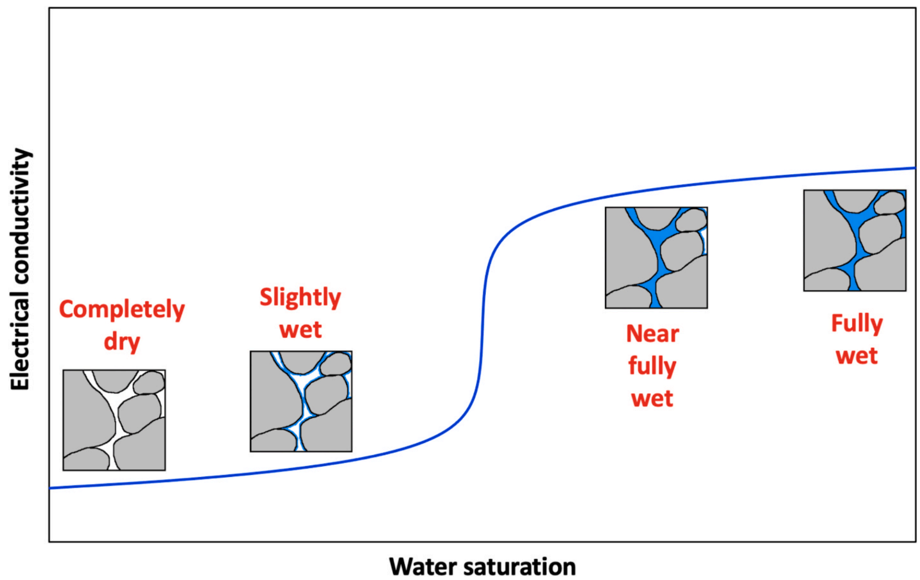

Fig. 1. Schematic saturation-dependent electrical conductivity in a porous medium. At low water saturations, surface conduction is dominant over bulk conduction due to lack of a continuous path of bulk water spanning the entire medium. At some critical water saturation, S_{wc}, a sample spanning cluster forms. Above the S_{wc} electrical conductivity mainly occurs through connected pores filled by water and bulk conduction becomes dominant over surface conduction.

simulated values from various publications (see their Table 1). In this study, we selected datasets which had significant surface conduction or σ_{dry} values. These selected data sets include data from Kechavarzi and Soga (2002), Binley et al. (2001), Binley et al. (2002) and Cassiani et al. (2004).

Kechavarzi and Soga (2002) measured saturation-dependent of electrical conductivity in clean sand samples, whereas the Binley et al. (2001; 2002) measurements were made on sandstone samples. Cassiani et al. (2004) performed numerical simulations on an image of a sandstone sample in the presence of surface conduction. Further details can be found in the original publications.

3.1.3. *Roberts (2002)* dataset

Roberts (2002) measured the saturation dependence of electrical conductivity of Topopah Spring Tuff at several temperatures i.e., 23, 40, 65, and 95 °C under ambient pressure conditions. The electrical conductivity was measured under wetting (or imbibition) conditions. Measurements were made over a range of frequency from 10^2 to 10^6 Hz. However, in this study only the measurements at 1 kHz were digitized and analyzed. The porosity of the sample was reported as 0.09 (9%).

3.1.4. *Ren et al. (1999)* dataset

Ren et al. (1999) used thermo-TDR sensors to measure saturation-dependent electrical conductivity in a clay loam sample with sand, clay and silt fractions of 0.37, 0.28 and 0.35, respectively. The soil sample was air dried, ground, and then passed through a 2-mm sieve. It was next moistened with distilled water having zero liquid electrical conductivity ($\sigma_f = 0$ dS/m) or with NaCl solutions corresponding to $\sigma_f =$ 0, 3, 6.9, 10.2, 14.3, and 21.9 dS/m to reach various water saturations. The electrical conductivity of the solutions was measured using a four-electrode probe. The soil samples were then mixed and packed into cylinders with internal diameter of 5.2 cm and height of 6.0 cm. The bulk density of the packed samples ranged from 1.05 to 1.10 g/cm^3.

For the Ren et al. (1999) dataset, we fitted the percolation-based effective-medium approximation to the saturation-dependent σ values measured in soil samples mixed with liquids with various electrical conductivity values i.e., 0, 3, 6.9, 10.2, 14.3, and 21.9 dS/m.

3.2. *Fitting the percolation-based effective medium approximation*

To fit the percolation-based effective medium approximation model and optimize its parameters for each data set, we first rearranged Eqs. (1) and (2) to have the fraction of high-conductivity component, f_h, and water saturation, S_w, as a function of the other parameters as follows (Ghanbarian and Daigle, 2016)

$$f_h = \frac{\left(\sigma^{1/t} - \sigma_l^{1/t}\right)\left[f_{hc}\sigma_h^{1/t} + (1 - f_{hc})\sigma^{1/t}\right]}{\left(\sigma_h^{1/t} - \sigma_l^{1/t}\right)\sigma^{1/t}} \tag{5}$$

$$S_w = \frac{\left(\sigma^{1/t} - \sigma_{dry}^{1/t}\right)\left[S_{wc}\sigma_{sat}^{1/t} + (1 - S_{wc})\sigma^{1/t}\right]}{\left(\sigma_{sat}^{1/t} - \sigma_{dry}^{1/t}\right)\sigma^{1/t}} \tag{6}$$

Eqs. (5) and (6) were then fitted to the $\sigma - f_h$ and/or $\sigma - S_w$ data. More specifically, we fitted Eq. (5) to the data from the Gostick and Weber (2015) dataset and Eq. (6) to the data from other datasets i.e., Ewing and Hunt (2006), Roberts (2002) and Ren et al. (1999). Recall that in the Gostick and Weber (2015) dataset the simulated σ values were reported at each volume fraction of the high-conductivity component, not for water saturation values. The fitting process was performed using the Curve Fitting toolbox of MATLAB.

4. Results

In this section, we present the obtained results and discuss them in detail for each dataset.

4.1. *Gostick and Weber (2015)*

Plots of the P-EMA model, Eq. (1), fitted to the site and bond percolation simulations from Gostick and Weber (2015) are presented in Fig. 2. Both curves are clearly, as expected, sigmoidal. Recall that in these simulations, σ_l was fixed at 0.001 S/m and $\sigma_h = 100$ S/m, and only the value of parameters t and f_{hc} were optimized by directly fitting Eq. (5) to the simulated values. In both site and bond percolation cases, we found very similar scaling exponents $t = 1.19$ for the site percolation (Fig. 2a) and 1.12 for the bond percolation (Fig. 2b), both less than the universal scaling exponent $t = 2$ in three dimensions (Sahimi, 2011).

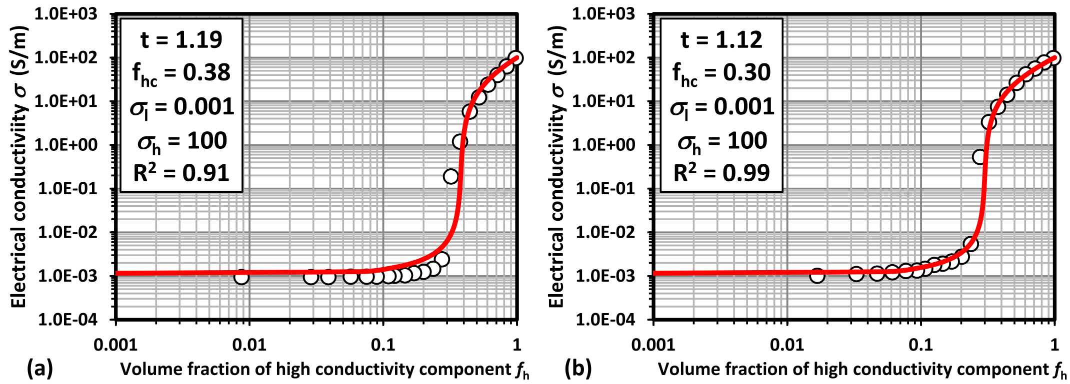

Fig. 2. Electrical conductivity versus the volume fraction of the high-conductivity component for (a) site percolation, and (b) bond percolation simulations from Gostick and Weber (2015) dataset. The red solid curves represent fits of Eq. (1) to the simulated values.

These exponents are also less than 1.9 (site percolation) and 1.5 (bond percolation) reported by Gostick and Weber (2015) who set $f_{hc} = 0.31$ for site and $f_{hc} = 0.2488$ for bond percolation, fitted the simple power law $\sigma \propto (f_h - f_{hc})^t$ to their simulations, and optimized the value of t. The discrepancy between exponents 1.19 and 1.12 from this study and 1.9 and 1.5 from Gostick and Weber (2015) is due to: (1) different mathematical forms used to determine the exponent t and (2) fixing the value of f_{hc} by Gostick and Weber (2015).

The percolation threshold $f_{hc} = 0.38$ for the site percolation (Fig. 2a) is greater than $f_{hc} = 0.30$ for the bond percolation (Fig. 2b). This is consistent with theoretical concepts of percolation theory where the percolation threshold for site percolation is expected to be greater than that for bond percolation on the same lattice (Hunt et al., 2014).

These values are also slightly greater than 0.31 for site and 0.2488 for bond percolation (Stauffer and Aharony, 1994) reported for insulator-conductor systems where only one conducting component exists.

4.2. Ewing and Hunt (2006)

Results presented in Fig. 3 demonstrate how well the P-EMA, Eq. (2), fits both the measured and simulated values from the Ewing and Hunt (2006) database. From model fits to the Kechavarzi and Soga (2002) measurements, we obtain $t = 0.44$, $S_{wc} = 0.32$, $\sigma_{dry} = 0.092$ S/m, and $\sigma_{sat} = 0.985$ S/m with $R^2 = 0.97$ (Fig. 3a). For the Binley et al. (2001) data, the optimized parameters are $t = 2.22$, $S_{wc} = 0.06$, $\sigma_{dry} = 0.012$ S/m, and $\sigma_{sat} = 0.173$ S/m with $R^2 = 0.98$ (Fig. 3b). These values are similar to $t = 2.39$, $S_{wc} = 2.6 \times 10^{-5}$, $\sigma_{dry} = 0.013$ S/m, and $\sigma_{sat} = 0.162$ S/m reported for the Binley et al. (2002) measured values (Fig. 3c). Recall that both Binley et al. (2001) and Binley et al. (2002) measured σ in sandstones. The large t values (2.22 and 2.39) in these two datasets are due to the upward curvature of the saturation-dependent electrical conductivity data similar to those in media with negligible surface conduction or insulator-conductor systems (see e.g., Mawer et al., 2015). Very small S_{wc} values (0.06 and 2.6×10^{-5}) also confirm that bulk conduction became dominant over surface conduction at very low values of water saturation.

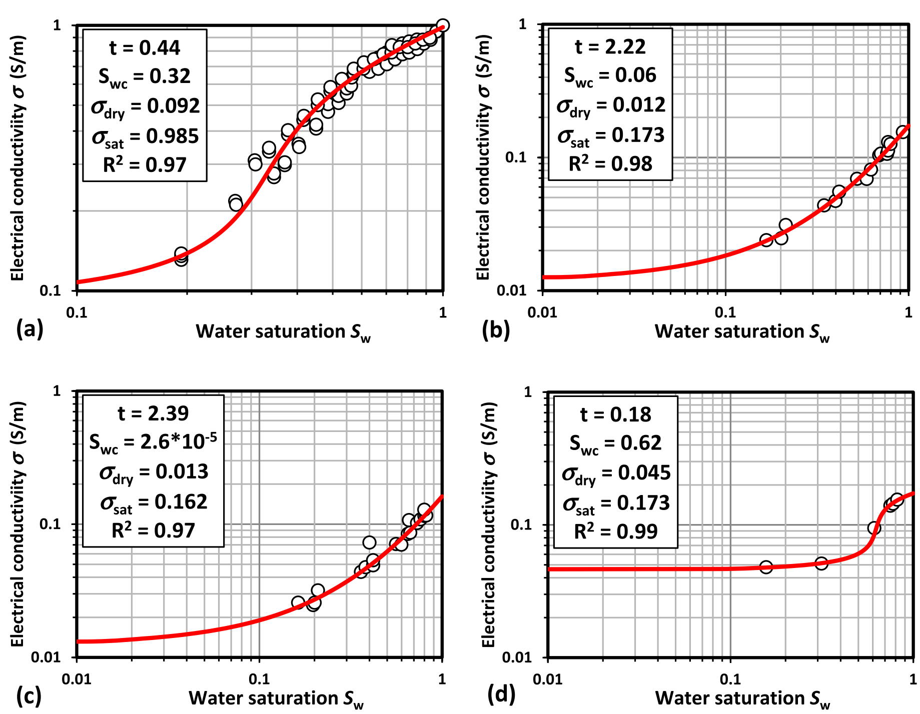

Fig. 3. Saturation dependence of electrical conductivity for the (a) Kechavarzi and Soga (2002), (b) Binley et al. (2001), (c) Binley et al. (2002), and (d) Cassiani et al. (2004) datasets. The red solid curves represent fits of Eq. (2) to the measured values.

For the Cassiani et al. (2004) simulated values we obtained $t = 0.18$, $S_{wc} = 0.62$, $\sigma_{dry} = 0.045$ S/m, and $\sigma_{sat} = 0.173$ S/m with $R^2 = 0.99$ (Fig. 3d). The value of $S_{wc} = 0.62$ for the Cassiani et al. (2004) simulation is the largest value among all of the datasets. Recently, Fu et al. (2024) reported a strong correlation between S_{wc} and water saturation at the inflection point of a capillary pressure curve using thermal conductivity measurements. Since Cassiani et al. (2004) reported simulated capillary pressures for their same sandstone sample, we digitized the capillary pressure curve corresponding to the sample volume (i.e., 384^3 voxels) used in the σ simulations from their Fig. 1. We calculated the water saturation at the inflection point on the simulated capillary pressure curve and found $S_w = 0.54$, which is fairly similar to $S_{wc} = 0.62$ (Fig. 3d).

4.3. Roberts (2002)

Fits of the P-EMA model, Eq. (2), to Topopah Spring Tuff sample measured values from Roberts (2002) are shown in Fig. 4. The measurements at low S_w values are rather scattered. For the data at 23 °C the optimized parameters are $t = 0.98$, $S_{wc} = 0.13$, $\sigma_{dry} = 7.9 \times 10^{-8}$ S/m, and $\sigma_{sat} = 1.9 \times 10^{-3}$ S/m with $R^2 = 0.87$ (Fig. 4a). For the data at 40 °C, the optimized parameters are $t = 0.83$, $S_{wc} = 0.12$, $\sigma_{dry} = 1.9 \times 10^{-7}$ S/m, and $\sigma_{sat} = 2.7 \times 10^{-3}$ S/m with $R^2 = 0.97$ (Fig. 4b). At 65 °C, fitting the P-EMA model results in $t = 0.74$, $S_{wc} = 0.13$, $\sigma_{dry} = 1.5 \times 10^{-7}$ S/m, and $\sigma_{sat} = 4.4 \times 10^{-3}$ S/m with $R^2 = 0.97$ (Fig. 4c). For data at 95 °C, the optimized values are $t = 1.27$, $S_{wc} = 0.10$, $\sigma_{dry} = 4.0 \times 10^{-8}$ S/m, and $\sigma_{sat} = 1.3 \times 10^{-2}$ S/m with $R^2 = 0.98$ (Fig. 4d). Thus, S_{wc} did not change as the temperature increased from 23 to 65 °C. However, its value decreased when the temperature was increased to 95 °C, indicating some high temperature structural change.

The scaling exponent t decreased from 0.98 to 0.74 as the temperature increased to 95 °C, which was a further indication of a structural change at 95 °C. The temperature dependence of the P-EMA model was also reported by Ghanbarian and Daigle (2016) who analyzed soil thermal conductivity measurements. They found by increasing temperature from 25 °C to 45 °C the value of thermal conductivity under completely dry and fully saturated conditions increased (see their Fig. 7). They also reported that S_{wc} decreased as temperature increased. For two out of three soil samples analyzed by Ghanbarian and Daigle (2016), the scaling exponent t value increased as temperature increased from 25 °C to 45 °C.

4.4. Ren et al. (1999)

Results of fitting the P-EMA model, Eq. (2), to the experimental data from Ren et al. (1999) are presented in Fig. 5. As can be observed, the P-EMA model fit the data well ($R^2 > 0.95$). For the clay loam soil sample saturated with the solution of zero salinity ($\sigma_f = 0$ dS/m), $t = 0.33$, $S_{wc} = 0.29$, $\sigma_{dry} = 0.024$ dS/m, and $\sigma_{sat} = 0.469$ dS/m with $R^2 = 0.99$ (Fig. 5a). Optimizing the P-EMA model parameters for the measured values with a σ_f of 3 dS/m resulted in $t = 0.88$, $S_{wc} = 0.22$, $\sigma_{dry} = 0.004$ dS/m, and $\sigma_{sat} = 1.680$ dS/m with $R^2 = 0.95$ (Fig. 5b). For the measured values with $\sigma_f = 6.9$ dS/m, $t = 1.39$, $S_{wc} = 0.17$, $\sigma_{dry} = 0.003$ dS/m, and $\sigma_{sat} = 3.850$ dS/m with $R^2 = 0.99$ (Fig. 5c). For the added solution with $\sigma_f = 10.2$ dS/m, fitting the P-EMA model resulted in $t = 1.05$, $S_{wc} = 0.22$, $\sigma_{dry} = 0.005$ dS/m, and $\sigma_{sat} = 5.11$ dS/m with $R^2 = 0.97$ (Fig. 5d). The optimized parameters of the P-EMA model were $t = 0.92$, $S_{wc} = 0.21$, $\sigma_{dry} = 0.005$ dS/m, and $\sigma_{sat} = 6.00$ dS/m with $R^2 = 0.96$ for $\sigma_f = 14.3$ dS/m (Fig. 5e). For the measured values in soil with the largest NaCl concentration ($\sigma_f = 21.9$ dS/m), we found $t = 1.04$, $S_{wc} = 0.20$, $\sigma_{dry} = 0.001$ dS/m, and $\sigma_{sat} = 9.280$ dS/m with $R^2 = 0.95$ (Fig. 5f).

Interestingly, the value of S_{wc} did not vary greatly among the measured values with non-zero-salinity solutions ($\sigma_f > 0$). The minimum value of $\sigma_{sat}/\sigma_{dry} = 19.5$ corresponded to the measured values with

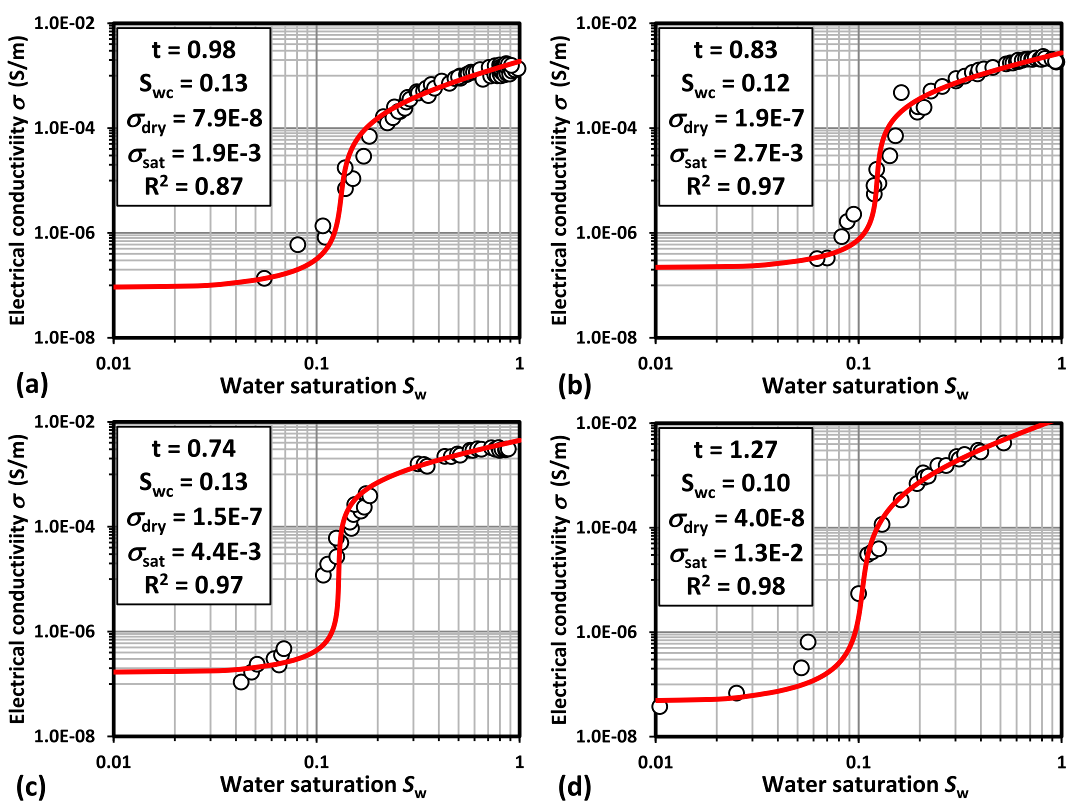

Fig. 4. Saturation dependence of electrical conductivity measured under wetting conditions at temperatures (a) 23 °C, (b) 40 °C, (c) 65 °C, and (d) 95 °C for the Topopah Spring tuff sample with porosity 0.09 from Roberts (2002). The red solid curves represent fits of Eq. (2) to the measured values.

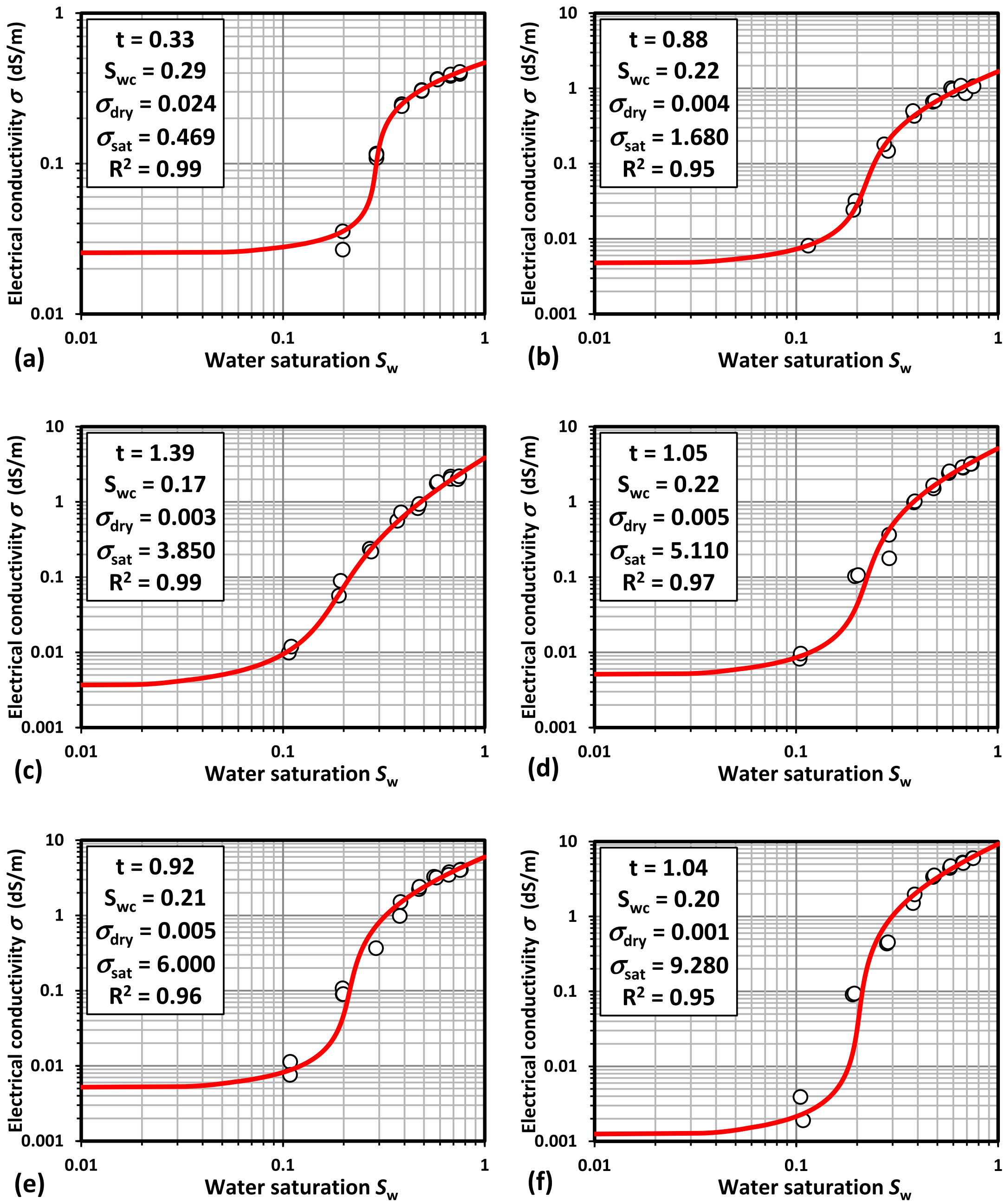

Fig. 5. Saturation dependence of electrical conductivity for clay loam soil samples from Ren et al. (1999) saturated with NaCl solutions σ_f with (a) 0 dS/m, (b) 3 dS/m, (c) 6.9 dS/m, (d) 10.2 dS/m, (e) 14.3 dS/m, and (f) 21.9 dS/m. The red solid curves represent fits of Eq. (2) to the measured values.

the zero-salinity solution ($\sigma_f = 0$ dS/m). As the σ_f value increased from 0 to 21.9 dS/m, the ratio of σ_{sat} to σ_{dry} increased substantially from 19.5 to 9280. The value of σ_{sat} increased remarkably from 0.469 to 9.28 dS/m, while the value of σ_{dry} decreased from 0.024 to 0.001 dS/m, as σ_f increased from 0 to 21.9 dS/m.

We also observed that σ_{sat} increased linearly with increasing σ_f for the non-zero-salinity solution experiments; $\sigma_{sat} = 0.44\,\sigma_f$ with $R^2 = 0.99$ (results not shown). Such a linear relationship has been observed by Bernabe and Revil (1995), Revil (2002), and others, at high enough σ_f values, and modeled by Waxman and Smith (1968), Qi and Wu (2022), among others. It, particularly at large σ_f, indicates that one can estimate the value of σ_{sat} at $\sigma_f = 6.9$ dS/m or higher values from a known σ_{sat} value at $\sigma_f = 3$ dS/m. This approximation to estimate the saturation dependence of σ with the P-EMA model is presented in the next section.

4.5. Estimating saturation-dependent σ via P-EMA

To demonstrate the usefulness of the percolation-based effective-medium approximation, we estimated the saturation dependence of σ at $\sigma_f = 6.9$, 10.2, 14.3 and 21.9 dS/m via Eq. (2) after setting $t = 0.88$, $S_{wc} = 0.22$ and $\sigma_{dry} = 0.004$ S/m determined by fitting the P-EMA model to the measurements at $\sigma_f = 3$ dS/m (Fig. 5b). As stated earlier, we observed a linear relationship between σ_{sat} and σ_f in the soil samples mixed with liquids with various electrical conductivity values, $\sigma_f = 3$, 6.9, 10.2, 14.3 and 21.9 dS/m. The value of σ_{sat} was accordingly estimated using the relationship $\sigma_{sat}(\sigma_f) = 1.68\frac{\sigma_f}{3}$ in which 1.68 dS/m is the σ_{sat} value at $\sigma_f = 3$ dS/m (Fig. 5b). This resulted in estimated values of $\sigma_{sat} = 3.85$, 5.70, 7.99 and 12.20 dS/m, not greatly different from the optimized values 3.85, 5.11, 6.00 and 9.28 dS/m reported in Fig. 5.

The estimated saturation-dependent σ values obtained with Eq. (2) at

$\sigma_f = 6.9$, 10.2, 14.3 and 21.9 dS/m are shown in blue in Fig. 6. As can be seen, the P-EMA produced reasonable estimations. One should bear in mind that the soil samples from Ren et al. (1999) were disturbed samples with a narrow range of bulk density (1.05–1.10 g/cm^3). However, bulk density is a macroscopic quantity, and similar bulk density values do not necessarily assure similar microscopic pore space characteristics, such as pore size distribution and pore connectivity. One should expect more accurate estimations by P-EMA if numerical simulations are performed for assumed soil images saturated with chemical solutions of various concentrations, because without strong dispersion/flocculation the pore space properties will not vary from one solution concentration to another.

5. Discussion

As demonstrated in Figs. 2-5, the P-EMA well characterized the saturation dependence of σ across the entire range of saturation from 0 (completely dry) to 1 (fully saturated). We found that the critical scaling exponent varied from 0.18 to 2.39 indicating non-universal scaling behavior in the saturation-dependent σ. Recall that $t = 2$ in three dimensions corresponds to the universal scaling (Stauffer and Aharony, 1994). The observed deviation from $t = 1$ ($0.18 \leq t \leq 2.39$) suggests that the effective-medium approximation, Eq. (2) with $t = 1$ and $f_{hc} = \frac{2}{Z}$, fails to accurately capture the nonlinear behavior of σ with changing saturation.

Furthermore, the small but non-zero values of σ_{dry} reported in Figs. 2-5 further indicate that the P-EMA did not reduce to the power-law scaling from percolation theory. This highlights important practical implications for porous media where surface conduction is significant.

The P-EMA, as expressed in Eqs. (1) and (2), was applied here for the first time to model the saturation dependence of electrical conductivity in porous media with surface conduction. We demonstrated that it fitted the experimental measurements and numerical simulations well. Additionally, we successfully evaluated its predictive capability using the experimental data from Ren et al. (1999). Nonetheless, similar to any other model, the P-EMA has its limitations.

For the Ren et al. (1999) dataset, we found $\sigma_{dry} = 0.024$ dS/m for the zero-concentration solution $\sigma_f = 0$ dS/m (Fig. 4a). This value is nearly one order of magnitude greater than that for the non-zero-salinity solutions (Fig. 4b-f), which is most probably due to a lack of measurements at low water saturations ($S_w < 0.1$). Accurately determining the values of the P-EMA model parameters requires precise measurements and/or simulations of σ over a broad range of S_w from zero (completely dry) to one (full saturation). Lack of data, particularly near $S_w = 0$, causes uncertainties in the determination of σ_{dry}. We should point out that measuring σ_{dry} in porous media is also challenging due to absence of reliable contact between solid grains and sensor. Similarly, if measurements and/or simulations are not available either around the percolation threshold (S_{wc}) or close to full saturation ($S_w = 1$), optimizing the P-EMA model parameters by fitting it to data may lead to inaccurate determination of S_{wc} or σ_{sat}.

Sadeghi et al. (2018), Fu et al. (2023; 2024) and Ore et al. (2024) reported that thermal conductivity P-EMA model parameters could be estimated from selected soil properties. For instance, Sadeghi et al. (2018) linked the scaling exponent t and critical water saturation S_{wc} to clay content in soils. However, further investigations are required to explore such correlations for electrical conductivity measurements.

6. Conclusions

For the first time, a percolation-based effective-medium approximation (P-EMA), Eq. (2), was applied to model electrical conductivity, σ,

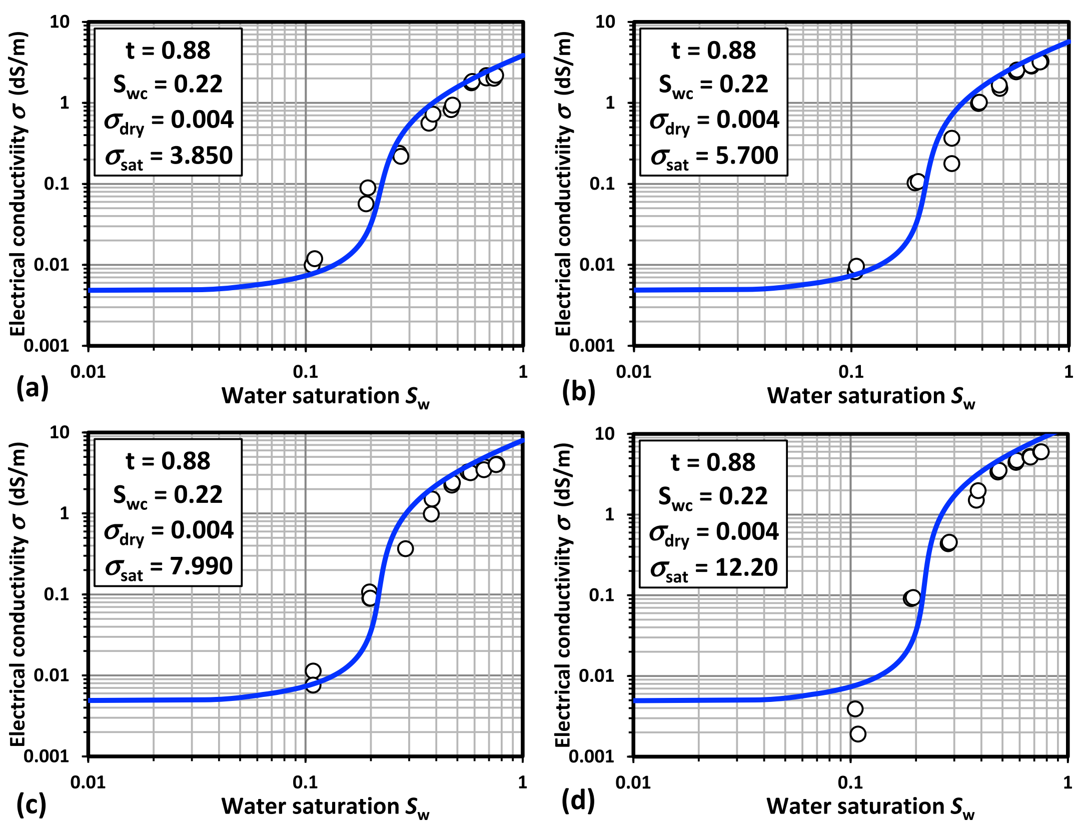

Fig. 6. Saturation dependence of electrical conductivity estimated via Eq. (2) for clay loam soil samples from Ren et al. (1999) saturated with NaCl solutions corresponding to (a) $\sigma_f = 6.9$ dS/m, (b) $\sigma_f = 10.2$ dS/m, (c) $\sigma_f = 14.3$ dS/m, and (d) $\sigma_f = 21.9$ dS/m. The parameters $t = 0.88$, $S_{wc} = 0.22$ and $\sigma_{dry} = 0.004$ S/m were obtained from fitting Eq. (2) to the $\sigma_f = 3$ dS/m experiment shown in Fig. 5b. The value of σ_{sat} was estimated from the product of $\sigma_{sat} = 1.680$ S/m (Fig. 5b) and the ratio of the σ_f values.

in porous media with significant surface conduction. The proposed model was evaluated using 3 numerically simulated datasets and 13 measured datasets. For this purpose, the model was directly fitted to the datasets, and the P-EMA model parameters were optimized. There was excellent agreement between the model and the data. More specifically, we found that the scaling exponent t ranged from 0.18 to 2.39, and the critical water saturation varied between 2.6×10^{-5} and 0.62. To assess usefulness of the model it was used to estimate saturation-dependent σ values for four soil samples mixed with liquids with various electrical conductivity values $\sigma_f = 6.9$, 10.2, 14.3 and 21.9 dS/m. There was reasonable agreement between the estimated and measured values. Future investigations are planned to investigate the correlation between t or S_{wc} and pore space charactersitics.

CRediT authorship contribution statement

David McLachlan: Writing – original draft, Validation, Methodology, Investigation, Conceptualization. **Meysam Ramezani:** Visualization, Validation, Methodology, Investigation, Formal analysis. **Robert Horton:** Writing – original draft, Validation, Supervision, Investigation, Conceptualization. **Behzad Ghanbarian:** Writing – original draft, Visualization, Validation, Supervision, Methodology, Investigation, Formal analysis, Conceptualization, Writing – review & editing.

Declaration of competing interest

The authors declare that they have no known competing financial interests or personal relationships that could have appeared to influence the work reported in this paper.

Acknowledgment

The authors acknowledge Dr. Tusheng Ren, China Agricultural University, for sharing data reported by Ren et al. (1999) and Dr. Robert Ewing, Climate LLC, for sharing Kechavarzi and Soga (2002), Binley et al. (2001), Binley et al. (2002) and Cassiani et al. (2004) and Roberts (2002) datasets, used in this study. BG acknowledges the University of Texas at Arlington for financial supports through faculty startup funds and a STARs award. RH acknowledges the National Science Foundation (2037504) and USDA-NIFA Multi-State Project 5188.

Data availability

Data are publicly available at McLachlan et al. (2025).

References

Adler, P.M., Berkowitz, B., 2000. Effective medium analysis of random lattices. Transp. Porous Media 40, 145–151.
Agbaje, T.Q., Ghanbarian, B., Hyman, J.D., 2023. Effective permeability in fractured reservoirs: Discrete fracture matrix simulations and percolation-based effective-medium approximation. Water Resour. Res. 59 (11), e2023WR036505.
Archie, G.E., 1942. The electrical resistivity log as an aid in determining some reservoir characteristics. Transactions of the AIME 146 (01), 54–62.
Bernabé, Y., Revil, A., 1995. Pore-scale heterogeneity, energy dissipation and the transport properties of rocks. Geophys. Res. Lett. 22 (12), 1529–1532.
Binley, A., P. Winship, R. Middleton, M. Pokar, and L.J. West. (2001). Observation of seasonal dynamics in the vadose zone using bore-hole radar and resistivity. In Proc. Symp. Appl. of Geophysics to Environ. and Eng. Problems (SAGEEP2001), Denver. 4–7 Mar. 2001. (On CD-ROM.) Environ. and Eng. Geophys. Soc., Denver, CO.
Binley, A., Winship, P., West, L.J., Pokar, M., Middleton, R., 2002. Seasonal variation of moisture content in unsaturated sandstone inferred from borehole radar and resistivity profiles. J. Hydrol. 267 (3–4), 160–172.
Cassiani, G., Dalla, E., Brovelli, A., Pitea, D., 2004. Pore-Scale Modeling of Electrical Conductivity in Unsaturated Sandstones Vol. 55, 235–245.
Doetsch, J., Linde, N., Pessognelli, M., Green, A.G., Günther, T., 2012. Constraining 3-D electrical resistance tomography with GPR reflection data for improved aquifer characterization. J. Appl. Geophys. 78, 68–76.
Ewing, R.P., Hunt, A.G., 2006. Dependence of the electrical conductivity on saturation in real porous media. Vadose Zone J. 5 (2), 731–741.
Fu, Y., Ghanbarian, B., Horton, R., Heitman, J., 2023. Robust calibration and evaluation of a percolation-based effective-medium approximation model for thermal conductivity of unsaturated soils. Geoderma 438, 116631.
Fu, Y., Ghanbarian, B., Horton, R., Heitman, J., 2024. New insights into the correlation between soil thermal conductivity and water retention in unsaturated soils. Vadose Zone J. 23 (1), e20297.
Ghanbarian, B., Daigle, H., 2016. Thermal conductivity in porous media: Percolation-based effective-medium approximation. Water Resour. Res. 52 (1), 295–314.
Ghanbarian, B., Berg, C.F., 2017. Formation factor in Bentheimer and Fontainebleau sandstones: Theory compared with pore-scale numerical simulations. Adv. Water Resour. 107, 139–146.
Ghanbarian, B., Sahimi, M., 2017. Electrical conductivity of partially saturated packings of particles. Transp. Porous Media 118 (1), 1–16.
Ghanbarian, B., Hunt, A.G., Ewing, R.P., Skinner, T.E., 2014. Universal scaling of the formation factor in porous media derived by combining percolation and effective medium theories. Geophys. Res. Lett. 41 (11), 3884–3890.
Gostick, J.T., Weber, A.Z., 2015. Resistor-network modeling of ionic conduction in polymer electrolytes. Electrochim. Acta 179, 137–145.
Hashin, Z., 1968. Assessment of the self consistent scheme approximation: conductivity of particulate composites. J. Compos. Mater. 2 (3), 284–300.
Hunt, A., Ewing, R., Ghanbarian, B., 2014. Percolation Theory for Flow in Porous Media, Vol. 880. Springer.
Johnson, D.L., Sen, P.N., 1988. Dependence of the conductivity of a porous medium on electrolyte conductivity. Phys. Rev. B 37 (7), 3502.
Karim, M.Z., Tucker-Kulesza, S.E., 2018. Predicting soil erodibility using electrical resistivity tomography. Journal of Geotechnical and Geoenvironmental Engineering 144 (4), 04018012.
Kechavarzi, C., Soga, K., 2002. Determination of water saturation using miniature resistivity probes during intermediate scale and centrifuge multiphase flow laboratory experiments. Geotech. Test. J. 25, 95–103.
Landauer, R., 1952. The electrical resistance of binary metallic mixtures. J. Appl. Phys. 23 (7), 779–784.
Last, B.J., Thouless, D.J., 1971. Percolation theory and electrical conductivity. Phys. Rev. Lett. 27 (25), 1719–1721.
Leroy, P., Revil, A., 2009. A mechanistic model for the spectral induced polarization of clay materials. J. Geophys. Res. Solid Earth 114 (B10).
Li, M., Tang, Y., Bernabé, Y., Zhao, J.Z., Li, X.F., Bai, X.Y., Zhang, L.H., 2015. Pore connectivity, electrical conductivity, and partial water saturation: network simulations. J. Geophys. Res. Solid Earth 120 (6), 4055–4068.
Martínez-Pagán, P., Gómez-Ortiz, D., Martín-Crespo, T., Manteca, J.I., Rosique, M., 2013. The electrical resistivity tomography method in the detection of shallow mining cavities. A case study on the Victoria Cave, Cartagena (SE Spain). Eng. Geol. 156, 1–10.
Mawer, C., Knight, R., Kitanidis, P.K., 2015. Relating relative hydraulic and electrical conductivity in the unsaturated zone. Water Resour. Res. 51 (1), 599–618.
McLachlan, D.S., 1985. Equation for the conductivity of metal-insulator mixtures. J. Phys. C Solid State Phys. 18 (9), 1891–1897.
McLachlan, D.S., 1987. An equation for the conductivity of binary mixtures with anisotropic grain structures. J. Phys. C Solid State Phys. 20 (7), 865–877.
McLachlan, D.S., 2021. The percolation exponents for electrical and thermal conductivities and the permittivity and permeability of binary composites. Phys. B Condens. Matter 606, 412658.
McLachlan, D., M. Ramezani, R. Horton, B. Ghanbarian (2025). Electrical conductivity in porous media with surface conduction, HydroShare, http://www.hydroshare.org/resource/437a93f43ca848768d3b673394c0cf12.
Perrone, A., Lapenna, V., Piscitelli, S., 2014. Electrical resistivity tomography technique for landslide investigation: A review. Earth Sci. Rev. 135, 65–82.
Qi, Y., Wu, Y., 2022. Electrical conductivity of clayey rocks and soils: A non-linear model. Geophys. Res. Lett. 49 (10), e2021GL097408.
Ore, T., Ghanbarian, B., Bohne, K., Wessolek, G., 2024. Saturation dependence of thermal conductivity of soils: Classification and estimations. International Journal of Thermophysics 45 (6), 81.
Ren, T., Noborio, K., Horton, R., 1999. Measuring soil water content, electrical conductivity, and thermal properties with a thermo-time domain reflectometry probe. Soil Sci. Soc. Am. J. 63 (3), 450–457.
Revil, A., 2002. The hydroelectric problem of porous rocks: thermodynamic approach and introduction of a percolation threshold. Geophys. J. Int. 151 (3), 944–949.
Revil, A., Glover, P.W.J., 1997. Theory of ionic-surface electrical conduction in porous media. Phys. Rev. B 55 (3), 1757.
Revil, A., Glover, P.W.J., 1998. Nature of surface electrical conductivity in natural sands, sandstones, and clays. Geophys. Res. Lett. 25 (5), 691–694.
Richesson, S., Sahimi, M., 2021. Flow and transport properties of deforming porous media. II. Electrical conductivity. Transp. Porous Media 138 (3), 611–636.
Roberts, J.J., 2002. Electrical properties of microporous rock as a function of saturation and temperature. J. Appl. Phys. 91 (3), 1687–1694.
Sahimi, M., Hughes, B.D., Scriven, L.E., Davis, H.T., 1983. Real-space renormalization and effective-medium approximation to the percolation conduction problem. Phys. Rev. B 28 (1), 307–311.
Sahimi, M., 1995. Progress in percolation theory and its applications. Annual Rev. Comput. Phys. II, 175–241.
Sahimi, M., 2011. Flow and transport in porous media and fractured rock: from classical methods to modern approaches. John Wiley & Sons.
Sahimi, M., 2023. Applications of Percolation Theory. Springer. 680, pp.
Sen, P.N., Scala, C., Cohen, M.H., 1981. A self-similar model for sedimentary rocks with application to the dielectric constant of fused glass beads. Geophysics 46 (5), 781–795.

Sen, P.N., 1997. Resistivity of partially saturated carbonate rocks with microporosity. Geophysics 62 (2), 415–425.
Stauffer, D., Aharony, A., 1994. Introduction to percolation theory. Taylor and Francis, London.
Tiab, D., Donaldson, E.C., 2024. Petrophysics: Theory and practice of measuring reservoir rock and fluid transport properties. Elsevier.
Waxman, M.H., Smits, L.J.M., 1968. Electrical conductivities in oil-bearing shaly sands. Soc. Pet. Eng. J. 8 (2), 107–122.
Wu, J., McLachlan, D.S., 1997. Percolation exponents and thresholds obtained from the nearly ideal continuum percolation system graphite-boron nitride. Phys. Rev. B 56 (3), 1236–1248.
Zhou, D., Stenby, E.H., 1997. A percolation study of wettability effect on the electrical properties of reservior rocks. Transp. Porous Media 29, 85–98.